Int. J. Morphol.,
44(4):1448-1460, 2026.

Empagliflozin Attenuates Cardiac Injury in STZ-Induced Diabetic Rats by Modulating Aquaporins and α-Smooth Muscle Actin

La Empagliflozina Atenúa el Daño Cardíaco en Ratas Diabéticas Inducidas por STZ Mediante la Modulación de las Acuaporinas y la Actina α de Músculo Liso

Naser A ElSawy[1]; Sameerah Shaheen[2]; Ashraf Saleh[3]; Naief A Dahran[4]; Hawazen A AlGifry[5]; Hany A. Elkattawy[6,7]; Sahar K. Ali[6,8]; Rania Naguib[9]; Nada Mohamed Mohamed Soliman[1] & Ahmed Algazeery[10]

ELSAWY, N. A.; SHAHEEN, S.; SALEH, A.; DAHRAN, N. A.; ALGIFRY, H. A.; ELKATTAWY, H.A.; ALI, S. K.; NAGUIB, R.; SOLIMAN, N. M. M. & ALGAZEERY, A. Empagliflozin attenuates cardiac injury in STZ-induced diabetic rats by modulating aquaporins and a-smooth muscle actin. *Int. J. Morphol., 44(4)*:1448-1460, 2026.

SUMMARY: Diabetes mellitus (DM) is a chronic metabolic disorder characterized by persistent hyperglycemia, leading to progressive damage to multiple organs. Among the serious complications, diabetic cardiomyopathy (DCM) is increasingly recognized as a major contributor to diabetes-related cardiovascular mortality. Sodium-glucose co-transporter-2 (SGLT2) inhibitors, such as empagliflozin (EMP), are well established as glucose-lowering agents; however, their direct protective mechanisms on cardiac tissue remain incompletely understood. This study aimed to explore the cardioprotective and molecular modulatory roles of EMP in a rat model of DCM. Forty male albino rats (180–200 g) were divided into four groups (n=10): control, vehicle, diabetic, and diabetic treated with EMP (10 mg/kg/day) for eight weeks. Cardiac tissues were analyzed histologically and immunohistochemically for aquaporin and a-smooth muscle actin (a-SMA) expression. Molecular changes were further assessed by quantifying Prkn gene expression, a key regulator of mitophagy. Empagliflozin treatment markedly improved cardiac histoarchitecture and reduced oxidative stress biomarkers compared to untreated diabetic rats. Immunohistochemical analysis revealed significant downregulation of aquaporin and a-SMA expression. Additionally, EMP treatment upregulated Prkn mRNA expression, indicating enhanced mitophagy activity within cardiomyocytes. Empagliflozin exerts a distinct cardioprotective effect in diabetic rats by modulating aquaporin channels, cytoskeletal remodeling, and Prkn-mediated mitophagy. These findings provide new mechanistic insights into the direct cardiac benefits of SGLT2 inhibition, supporting EMP as a promising therapeutic target for diabetic cardiomyopathy.

KEY WORDS: Diabetic cardiomyopathy; SGLT2 inhibitor; Empagliflozin; Aquaporin; a-SMA; Mitophagy; Prkn.

INTRODUCTION

Diabetes mellitus (DM) comprises a group of metabolic disorders characterized by persistent hyperglycemia resulting from impaired insulin secretion, insulin action, or both (Loscalzo *et al*., 2022). Chronic elevation of blood glucose levels induces widespread vascular and tissue injury, contributing to serious complications affecting the cardiovascular system, kidneys, eyes, and peripheral nerves. According to the World Health Organization (WHO), diabetes affects more than 422 million individuals globally and directly accounts for approximately 1.5 million deaths each year (Sanjari *et al*., 2025). Among its systemic manifestations, the cardiovascular complications collectively termed diabetic

[1] Department of Anatomy & Embryology, Faculty of Medicine, Zagazig University, Zagazig, Egypt.
[2] Department of Anatomy and Stem Cell Unit, College of Medicine, King Saud University, Riyadh, Saudi Arabia.
[3] Physiology Department, Faculty of Medicine, Tobruk University, Tobruk, Libyan Arab Jamahiriya.
[4] Department of Basic Medical Sciences, College of Medicine, University of Jeddah, Jeddah, Saudi Arabia.
[5] Clinical Laboratory Sciences, Faculty of Applied Medical Sciences, Umm Al-Qura University, Makkah, Saudi Arabia.
[6] Department of Basic Medical Sciences, College of Medicine, AlMaarefa University, Diriyah, Riyadh, Saudi Arabia.
[7] Research Center, Deanship of Scientific Research and Postgraduate Studies, AlMaarefa University, Diriyah, Riyadh, Saudi Arabia.
[8] Department of Clinical Pharmacology, Faculty of Medicine, Zagazig University, Zagazig, Egypt.
[9] Department of Internal Medicine, College of Medicine, Princess Nourah bint Abdulrahman University, Riyadh, Saudi Arabia.
[10] Zoology Department, Faculty of Science, Zagazig University, Zagazig, Egypt.
FUNDING. Princess Nourah bint Abdulrahman University Researchers Supporting Project number (PNURSP2026R774), Princess Nourah bint Abdulrahman University, Riyadh, Saudi Arabia.

Received: 2026-04-24 Accepted: 2026-06-25

cardiomyopathy (DCM) represent a major cause of morbidity and mortality. DCM is characterized by myocardial fibrosis, cardiomyocyte hypertrophy, ventricular dysfunction, and structural heart remodeling, all of which contribute to progressive deterioration of cardiac performance (Balakrishnan *et al*., 2025).

Glucose transport in mammalian cells occurs via two main systems: facilitative glucose transporters (GLUTs) and sodium–glucose cotransporters (SGLTs). While GLUTs mediate passive glucose diffusion along concentration gradients, SGLTs actively transport glucose against this gradient through sodium coupling. Among the six known human SGLT isoforms, SGLT1 and SGLT2 are the most physiologically and pharmacologically relevant, playing key roles in glucose homeostasis and serving as major therapeutic targets in diabetes and metabolic disorders (Hirayama *et al*., 1991; Mueckler, 1994; Wright, 2001; Joost & Thorens, 2001; Wood & Trayhurn, 2003; Scheepers *et al*., 2004).

Current therapeutic strategies often address diabetic cardiomyopathy as a secondary complication of diabetes. Glucose-lowering agents, including glucagon-like peptide-1 (GLP-1) receptor agonists and sodium-glucose co-transporter 2 (SGLT2) inhibitors, remain the mainstay of treatment. SGLT2 inhibitors—such as canagliflozin, dapagliflozin, empagliflozin, and ertugliflozin—lower blood glucose by blocking renal glucose and sodium reabsorption in the proximal tubules, promoting urinary excretion. This insulin-independent mechanism not only improves glycemic control but also confers notable cardiovascular and renal protection, establishing SGLT2 inhibitors as key components of modern diabetes management (Wiviott *et al*., 2019).

Although the benefits of empagliflozin, including weight reduction and cardioprotection, are well established, most studies have evaluated its efficacy as a second-line therapy in combination with metformin and primarily in patients with uncontrolled diabetes or heart failure. Emerging evidence highlights its influence on energy metabolism, cardiac fibrosis, and electrolyte homeostasis (Bertero *et al*., 2018). Historically, phlorizin—first isolated from apple tree bark—was the earliest natural SGLT inhibitor with potent and selective activity against both SGLT1 and SGLT2. Initially used to treat infectious diseases, it was later observed to induce glycosuria, paving the way for the development of modern SGLT2 inhibitors (Ghezzi *et al*., 2018).

Despite the well-established renal and metabolic actions of sodium-glucose co-transporter-2 (SGLT2) inhibitors, the direct cardioprotective mechanisms of empagliflozin on myocardial tissue remain incompletely understood. To elucidate these mechanisms, the present study explored histopathological, immunohistochemical, and gene expression alterations associated with mitochondrial injury in diabetic cardiomyopathy. Specifically, we examined oxidative stress–related changes and their impact on the expression of two key markers: aquaporins (AQPs) and alpha-smooth muscle actin (a-SMA). AQPs are transmembrane channels widely expressed in various tissues, including cardiomyocytes, where they facilitate water movement along osmotic gradients (Agre, 2004; Egan *et al*., 2006; Rutkovskiy *et al*., 2013; Tie *et al*., 2017). In addition to water transport, certain AQPs are involved in the translocation of glucose across cell membranes (Arie *et al*., 2019). Excessive glucose flux through these channels leads to concomitant water influx, contributing to intracellular edema and cardiac dysfunction (Koepsell, 2020). Meanwhile, a-SMA, an actin-binding cytoskeletal protein abundantly expressed in vascular smooth muscle cells, plays a crucial role in maintaining extracellular matrix (ECM) structure; its dysregulation has been associated with maladaptive cardiac remodeling and fibrosis (Yuan & Wu, 2018).

To elucidate the molecular mechanisms underlying cardiomyocyte differentiation in response to empagliflozin treatment in a diabetic rat model, we examined the expression of mitophagy-related genes, with a focus on the Parkin (Prkn) pathway. This pathway has been implicated in mitochondrial quality control and cardiomyocyte homeostasis (Song *et al*., 2021). Notably, recessive loss-of-function mutations in Prkn are associated with impaired mitophagy and mitochondrial dysfunction (Mackey *et al*., 2017). Based on this evidence, we hypothesized that empagliflozin exerts cardioprotective effects in diabetic cardiomyopathy by modulating oxidative stress and enhancing Prkn-mediated mitophagy, thereby preserving mitochondrial integrity and improving cardiac histoarchitecture.

MATERIAL AND METHOD

Experimental Animals

Forty male albino rats, weighing 220-250 g, participated in the experiments. All animals were housed in accordance with the National Research Council's guidelines for the care and use of laboratory animals. During the study, the animals were housed in standard plastic cages at 21 ± 2 °C and 55 %-65 % humidity. They were subjected to a 12-hour light-dark cycle and had free access to standard rat chow and tap water (Mohamad *et al*., 2020). All procedures received approval from the Institutional Animal Care and Use Committee at Zagazig University, Egypt (approval number: ZU-IACUC/1/F/185/2025).

Chemicals

Empagliflozin (Jardiance, 25 mg; Boehringer Ingelheim) was suspended in 0.5 % hydroxyethyl cellulose (Sigma-Aldrich, St. Louis, MO, USA) and administered by oral gavage, while placebo animals received vehicle only (Bogdanffy *et al*., 2014). Streptozotocin was obtained from Sigma-Aldrich (St. Louis, MO, USA). Total RNA was extracted using TRIzol reagent (Invitrogen, Thermo Fisher Scientific, USA). Serum insulin levels were measured using a rat INS-EASIA kit (KAP1251; BioSource Europe S.A., Nivelles, Belgium). Cardiac superoxide dismutase (SOD) activity was assessed with a colorimetric assay kit (Invitrogen, SOD Colorimetric Activity Kit, Cat. No. EIASODC, USA). Creatine kinase-MB (CK-MB) levels were determined using a commercial kit (Pointe Scientific Inc., Canton, MI, USA). Troponin levels were measured using a standardized immunoassay kit according to the manufacturer's instructions. Fasting serum glucose levels were quantified by the hexokinase method on a Cobas Integra 400 Plus analyzer, following established protocols (Warade & Pandey, 2014).

Experimental Groups

A total of 40 adult albino rats were randomly allocated into four groups (n=10 per group). Group 1 (control) was maintained under standard laboratory conditions, received a standard chow diet, and was given oral vehicle (0.5 % hydroxyethyl cellulose) daily for 8 weeks. Group 2 (EMPA) was maintained under the same conditions and received empagliflozin at 10 mg/kg/day (Ekici *et al*., 2022), suspended in 0.5 % hydroxyethyl cellulose, and administered by oral gavage for 8 weeks, after which the animals were sacrificed. In Group 3 (STZ), type 2 diabetes mellitus was induced by a single intraperitoneal injection of streptozotocin (STZ, 50 mg/kg) dissolved in citrate buffer (Furman, 2021). After 48 h, rats with fasting blood glucose levels >250 mg/dL were considered diabetic and were followed until the end of the 8 weeks, when they were euthanized (Gheibi *et al*., 2017). Group 4 (STZ + EMPA) was rendered diabetic using the same STZ protocol, and rats with fasting blood glucose >250 mg/dL after 48 h were subsequently treated with empagliflozin (10 mg/kg/day in 0.5 % hydroxyethyl cellulose by oral gavage) for 8 weeks before sacrifice.

The empagliflozin dose was determined by adjusting for key pharmacokinetic differences and metabolic variations between rodents and humans, such as the shorter half-life of 1–2 hours in rodents versus 10–12 hours in humans. This dose has been previously shown to be effective and equivalent to active human doses (Steven *et al*., 2017).

Animal euthanasia and sample collection

Rats were euthanized by intraperitoneal injection of thiopental (12 mg/100 g body weight) following an overnight fast (Pang & Laferriere, 2020). Blood samples were obtained via cardiac puncture and collected into two tubes per animal. Subsequently, the heart was excised and processed according to the protocol described by Koay *et al*. (2025). The cardiac tissue was divided into three portions: a small segment of the left ventricle (50–100 mg) was immediately immersed in RNAlater solution (0.5–1 mL), kept at 2–8 °C overnight, and then stored at -80 °C for subsequent real-time PCR analysis. A second portion was weighed and rapidly snap-frozen in liquid nitrogen for biochemical assays. The remaining portion was fixed in 10 % formalin for histopathological and immunohistochemical evaluation.

Biochemical Procedure

Blood samples were collected from direct heart puncture after anesthesia had been administered to assess serum biochemical parameters. The blood was centrifuged at 3000 rpm for 5 minutes. The serum was then separated and divided into three microtubes (each containing 500 mL) and stored at -20 °C until further testing (Elkattawy *et al*., 2025).

Assessment of Serum Fasting Glucose, Insulin, and HOMA-IR

Serum glucose concentration was measured using an enzymatic colorimetric assay with a commercial glucose kit, and serum insulin levels were determined using a rat insulin ELISA kit, both according to the manufacturers' instructions (Elkattawy *et al*., 2023). Insulin resistance was estimated using the homeostatic model assessment for insulin resistance (HOMA-IR), calculated as follows: HOMA-IR = Fasting Blood Glucose (mg/dl) x Fasting Insulin (IU/ml) / 22.5. Then, the formula was applied directly, and glucose values were first converted to mmol/L before calculation using the Matthews *et al*., (1985) method.

Assessment of Cardiac Injury Biomarkers

Creatine kinase-MB (CK-MB) and troponin activity were determined using a kinetic spectrophotometric method originally described by Oliver (1955) and subsequently modified by Rosalki *et al*. (2004). Troponin levels were measured using a standardized immunoassay kit according to themanufacturer's instructions (Hassan *et al*., 2023).

Assessment of Cardiac Tissue Oxidative and Antioxidant Biomarkers

Cardiac superoxide dismutase (SOD) activity was measured according to the spectrophotometric method of Kakkar *et al*. (1984). Cardiac malondialdehyde (MDA), an index of lipid peroxidation, was quantified by the thiobarbituric acid (TBA) assay as described by Ohkawa *et al*. (1979), in which MDA reacts with TBA in an acidic medium at 95 °C for 30 min to form a TBA-reactive pink chromogen, the absorbance of which was measured at 534 nm using a spectrophotometer.

Molecular Expression Analysis of Cardiac-Related Genes

Total RNA was extracted from cardiac tissue using TRIzol reagent (Invitrogen, Thermo Fisher Scientific, USA). Approximately 30 mg of whole tissue was homogenized in 1 mL of TRIzol according to the protocol described by Livak & Schmittgen (2001). RNA purity and integrity were assessed using a NanoDrop® ND–1000 spectrophotometer (NanoDrop Technologies, Wilmington, DE, USA), and samples with an A260/A280 ratio of 1.8-2.0 were considered suitable for further analysis. RNA concentrations were determined spectrophotometrically at 260 nm. Complementary DNA (cDNA) was synthesized from 50 ng of total RNA using a High-Capacity cDNA Reverse Transcription Kit (Applied Biosystems™, USA) according to the manufacturer's instructions. The reverse transcription reaction was carried out in a total volume of 20 µL containing 5 µL of RNA (50 ng), 4 µL of 5× miRCURY RT reaction buffer, and 2.5 µL of 10× miRCURY RT enzyme mix (Qiagen, Germany). The reaction was incubated at 45?°C for 60?min, followed by enzyme inactivation at 85?°C for 10?min using a Biometra 96-well thermal cycler (Applied Biosystems). All primers were diluted in RNase/DNase-free water to the concentrations recommended by the manufacturer before use. Real-time RT-PCR was carried out on a Rotor-Gene Q 2plex Real-Time PCR System (Qiagen, Germany) using TOPreal™ qPCR 2X PreMIX (SYBR Green with low ROX; Cat. No. P725 or P750, Enzynomics, Korea), in accordance with the manufacturer's protocol (Table I).

Histopathological Analysis

Heart tissues were carefully excised, rinsed in saline to remove excess blood, and immediately fixed in 10 % neutral buffered formalin to preserve myocardial architecture. Following fixation, specimens were processed through a graded ethanol series for dehydration, cleared in xylene, and embedded in paraffin wax using standard histological techniques. Serial sections of 4 mm thickness were cut on a rotary microtome, mounted on glass slides, and stained with hematoxylin and eosin (H&E) for general histopathological evaluation using the method of Bancroft & Cook (1984).

Immunohistochemical (IHC) Analysis

To characterize the immunohistopathological alterations associated with diabetic cardiomyopathy and to assess the cardioprotective effects of empagliflozin, paraffin-embedded heart sections (4 mm thick) were subjected to immunohistochemical staining for aquaporin and a-smooth muscle actin (a-SMA). Sections were deparaffinized, rehydrated through graded alcohols, and processed for antigen retrieval, followed by incubation with specific monoclonal primary antibodies against aquaporin

Table I. primer sequences used for quantitative real-time PCR assay.

Gene	Primer Sequence (5'–3')	References
IL-8	**Forward (5'–3'):** CATTAATATTTAACGATGTGGATGCGTTTCA	NM_030845.1
	Reverse (5'–3'): GCCTACCATCTTTAAACTGCACAAT	
TGF-β1	**Forward (5'–3'):** GGAGCCACTGCCCATCGTCTACTAC	NM_021578.2
	Reverse (5'–3'): GGAGCGCACGATCATGTTGGAC	
TNF-α	**Forward (5'–3'):** ACTGAACTTCGGGGTGATCG	NM_012675.3
	Reverse (5'–3'): GCTTGGTGGTTTGCTACGAC	
NF-kB	**Forward (5'–3'):** CAGGACCAGGAACAGTTCGAA	NM_199267.2
	Reverse (5'–3'): CCAGGTTCTGGAAGCTATGGAT	
RAGE	**Forward (5'–3'):** TGCCCAGCCTCCCCCTCAAA	NM_053336.2
	Reverse (5'–3'): GGGTGGCCACGCAGCTGTAG	
PKC	**Forward (5'–3'):** AGCCGGAGTGGATGGCTGGT	NM_19007.1
	Reverse (5'–3'): CTCGCTTTCTTCCGGCGGCA	
PRKN	**Forward (5'–3'):** GAACTGTGGCTGTGAGTGGA	
	Reverse (5'–3'): GGTGTTTCCCATGAGGTCGT	NM_020093.1
GAPDH	**Forward (5'–3'):** GGCACAGTCAAGGCTGAGAATG	
	Reverse (5'–3'): ATGGTGGTGAAGACGCCAGTA	NM_017008.4

and a-SMA, as described by Samuel *et al*. (2007). Immunoreactivity was visualized using a horseradish peroxidase–conjugated detection system with diaminobenzidine (DAB) as the chromogen, yielding a brown cytoplasmic precipitate in positively stained cells, and nuclei were counterstained with hematoxylin for optimal tissue contrast.

Morphometric Analysis

Cardiac tissue sections stained with hematoxylin and eosin (H&E) were analyzed to quantify fibrotic areas using the measuring field menu. Random microscopic fields were examined at 100× magnification, with an average of 15 readings per animal and per group, resulting in a total of 90 measurements per group. H&E staining was performed on every 20th section of the cardiac tissue, with each section separated by approximately 50–60 μm to avoid repeated counting of the same region. Indicators of cardiac injury included interstitial edema, vascular dilation, fibrosis, hemorrhage, and infiltration of inflammatory cells. Tissue damage was graded on a semi-quantitative scale from 0 to 4, reflecting severity (0: none, 1: mild, 2: moderate, 3: severe, 4: very severe). A single blinded observer performed the scoring, evaluating at least five microscopic areas per specimen. Key assessment parameters encompassed histological evaluation of myocardial fibrosis (collagen deposition), cardiomyocyte hypertrophy, and structural remodeling characterized by increased interstitial fibrosis. Immunohistochemical results were quantified by morphometric analysis in ImageJ, measuring the percentage area of aquaporin and α-SMA immunoreactivity at high magnification (×400). Measurements were taken from randomly selected fields of rat cardiac tissues to reduce bias. Morphometric analysis of histopathological changes in H&E-stained sections and immunohistochemical expression will be performed using a light microscope (LEICA DM500) with a digital camera (Leica ICC50 W), Anatomy Department, Faculty of Medicine, Zagazig University. and Data were analyzed by "Image J 1.49v/ Java 1.6.0_244" (NIH, USA) Software.

Statistical Analysis

All data were collected, managed, and statistically analyzed using IBM SPSS Statistics for Windows, version 22.0 (IBM Corp., Armonk, NY, USA). Quantitative results are expressed as mean ± standard deviation (SD). Morphometric and image-based analyses were performed using GraphPad Prism software (version 8.4.3). Group differences were assessed using one-way analysis of variance (ANOVA), followed, where appropriate, by post hoc multiple-comparison tests to determine significance between groups. Data were considered significant when the p-value was < 0.05.

RESULTS

Effect on Serum Fasting Glucose, Insulin, and HOMA-IR

STZ administration markedly disrupted glycemic homeostasis, as evidenced by significant increases in fasting blood glucose, serum insulin, and HOMA-IR compared with the control group. The elevated HOMA-IR indicates the development of pronounced insulin resistance in the diabetic rats (Elkattawy *et al*., 2022). EMPA treatment partially improved these abnormalities, with reductions in fasting blood glucose, serum insulin, and HOMA-IR relative to the STZ group, suggesting an ameliorative effect on glucose metabolism and insulin sensitivity. However, the values in the STZ+EMPA group remained higher than in the control group, indicating partial rather than complete restoration of metabolic status (Table II).

Effect on Cardiac Injury Biomarkers

The results show that empagliflozin alone reduced serum troponin and CK-MB levels compared with the control group, whereas STZ markedly increased both cardiac injury markers. Treatment with EMPA markedly reduced troponin levels, restoring them to values comparable to those of the control group. However, CK-

Table II. Effects of administration of empagliflozin on serum fasting insulin, fasting blood glucose, and HOMA-IR in all groups.

	Control	EMPA	STZ	STZ+EMPA
Serum fasting insulin levels (μiu/ml)	20.8±1.76	18.5±1.13	25.9±1.29^{a,b}	22.4±1.76^{a,b,c}
Serum Fasting Blood Glucose (mg/dl)	98.5±5.55	98±5.26	376±48.55^{a,b}	266±34.75^{a,b,c}
HOMA- IR	6.06±0.3	6.1±0.43	19.15±0.99^{a,b}	12.98±1.33^{a,b,c}

Values are expressed as mean ± SD (10 rats per group). Superscripts indicate statistical significance at $P < 0.05$: a, *vs.* control group; b, *vs*. empagliflozin group; c, vs. STZ group.

MB levels in the EMPA group showed only partial recovery toward normal levels (Fig. 1).

Effect on Cardiac Tissue Oxidative / Antioxidative Markers

The control and EMPA-treated groups exhibited relatively stable levels of oxidative and antioxidant biomarkers. In contrast, STZ administration induced significant oxidative stress in cardiac tissue, as demonstrated by increased MDA levels and disrupted SOD activity ($p < 0.05$). Treatment with EMPA in the STZ+EMPA group significantly mitigated these changes, as evidenced by reduced MDA levels compared to the STZ group and a restoration of SOD activity toward normal levels (Fig. 2).

Effects on mRNA Expression of Pro-Inflammatory and Fibrosis Markers Related Genes

The control and EMPA groups showed similar expression levels of IL-8, NF-kB, TNF-a, TGF-b1, RAGE, PKC, and PRKN, indicating that EMPA alone did not significantly alter these markers. In contrast, STZ administration markedly increased the expression of all measured genes ($p < 0.05$), demonstrating activation of inflammatory, fibrotic, and stress-related pathways in the diabetic rats. Co-administration of EMPA with STZ reduced the elevated expression of these genes compared with the STZ group. However, the expression levels in the STZ+EMPA group remained higher than those of the control group, suggesting a partial protective effect of EMPA against STZ-induced molecular changes (Tables III and IV).

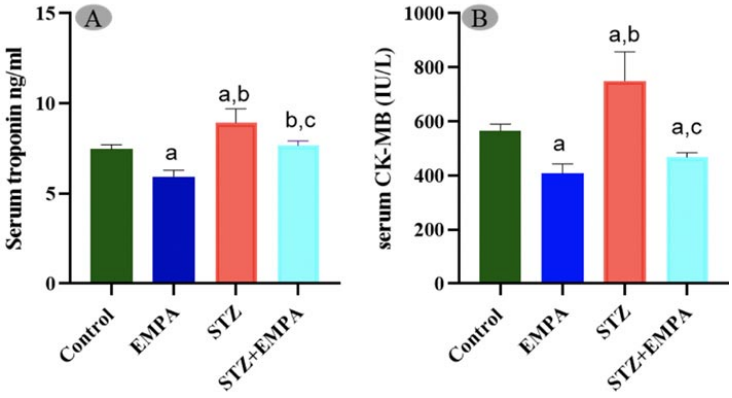


Fig. 1. Effects of co-administration of empagliflozin on serum troponin and CK-MB in all groups. Values are expressed as mean ± SD (10 rats per group). Superscripts indicate statistical significance at $P < 0.05$: a. *vs.* control group; b. *vs.* empagliflozin group; c. *vs.* STZ group.

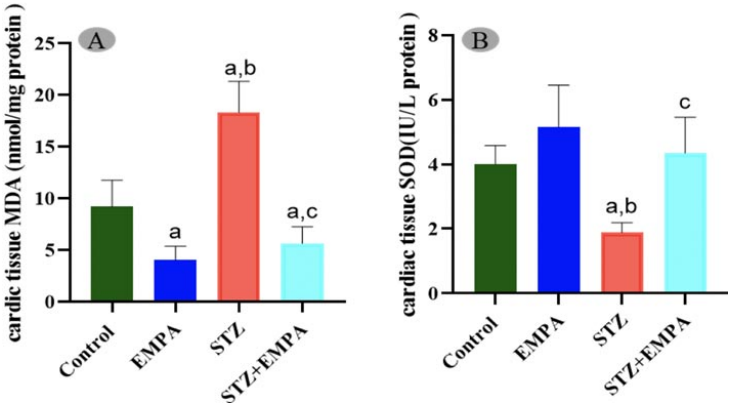


Fig. 2. Effects of co-administration of empagliflozin on cardiac tissue SOD and MDA levels in all groups. Values are expressed as mean ± SD (10 rats per group). Superscripts indicate statistical significance at $P < 0.05$: a. *vs.* control group; b. *vs.* empagliflozin group; c. *vs.* STZ group.

Table III. Effects of co-administration of empagliflozin on mRNA expression of pro-inflammatory and fibrosis markers related genes in STZ-induced diabetes in rats.

	Control	EMPA	STZ	STZ+EMPA
IL-8	1.09±0.04	1.14±0.12	1.57±0.17^{a,b}	1.29±0.11^{a,b,c}
NF-κB	1.02±0.06	1.04±0.09	1.47±0.13, c^{a,b}	1.24±0.16^{a,b,c}
TNF-α	1.03±0.05	1.1±0.07	1.39±0.19^{a,b}	1.24±0.09^{a,b,c}
TGF-β1	1.01±0.09	1.15±0.1	1.46±0.17^{a,b}	1.32±0.11^{a,b,c}
RAGE	1±0.09	1.69±1.18	5.91±1.18^{a,b}	3.74±0.17^{a,b,c}
PKC	1.01±0.05	1.21±0.12	1.39±0.29^{a,b}	1.22±0.15^{a,b,c}
PRKN	0.23±0.04	0.25±0.05	1.16±0.10^{a,b}	0.74±0.11^{a,b,c}

Values are expressed as mean ± SD (10 rats per group). Superscripts indicate statistical significance at $P < 0.05$: a, vs. control group; b, vs. empagliflozin group; c, vs. STZ group. IL-8; interleukin 8, NF-KB; nuclear factor kappa b, TNF-a; tumor necrosis factor alpha, TGF-b1; transforming growthfactor beta, RAGE; receptor for advanced glycation end products, PKC; protein kinase C, and PRKN; Parkin RBR E3 Ubiquitin Protein Ligase.

Histopathological Results

H&E-stained sections of the control group revealed bundles of branching and anastomosing cardiomyocytes separated by narrow spaces. Cardiomyocytes showed a regular outline, acidophilic sarcoplasm with visible cross-striations, and a centrally located vesicular nucleus. Inter-bundle spaces contained normal blood capillaries (Fig. 3A). The EMPA group showed preserved architecture with apparently small-sized cardiomyocytes, acidophilic sarcoplasm, and centrally located nuclei. Slightly wider interfibrillar spaces were observed compared to the control group (Fig. 3B).

H&E-stained sections of STZ groups demonstrated disruption of myocardial architecture with widened spaces between muscle fibers (M). Observations included inflammatory exudate, extensive hemorrhage, and severely congested blood vessels. Many cardiomyocytes exhibited fiber splitting, pale sarcoplasm with vacuolation, and darkly stained nuclei with chromatin margination. Deeply acidophilic cells with loss of striations and boxcar nuclei were also observed, indicating Zenker's degeneration (Fig. 4A-D).

H&E-stained sections of the left ventricle of the STZ+ EMPA group revealed slightly widened spaces and moderate splitting of the cardiomyocytes, accompanied by inflammatory cellular infiltrates between irregular, wavy-directed cardiomyocytes (Fig. 5A-D).

Immunohistochemical Results

Effect of EMPA on Aquaporin

Immunohistochemical staining for aquaporin in the control group showed minimal reactivity (Fig. 6A). A mild reaction was observed in the EMPA group (Fig. 6B). In contrast, the STZ group demonstrated a severe reaction (Fig. 6C). Notably, administration of empagliflozin moderately improved this reaction, as illustrated in Figure 6D.

Effect of EMPA on α-SMA

In the control group, immunohistochemical staining for a-SMA exhibited minimal expression (Fig. 7A). The EMPA group displayed a mild positive reaction (Fig. 7B). Marked staining intensity was evident in the STZ group (Fig. 7C). However, treatment with empagliflozin resulted in a moderate improvement in this reaction, as shown in Figure 7D.

DISCUSSION

Diabetic cardiomyopathy remains a major contributor to myocardial injury, in part through sustained intracellular hyperglycemia that accelerates the formation of advanced glycation end products and enhances reactive oxygen species (ROS) generation (Yuan *et al*., 2019). In this setting, excess free radicals attack membrane polyunsaturated fatty acids, triggering lipid peroxidation and amplifying oxidative stress,

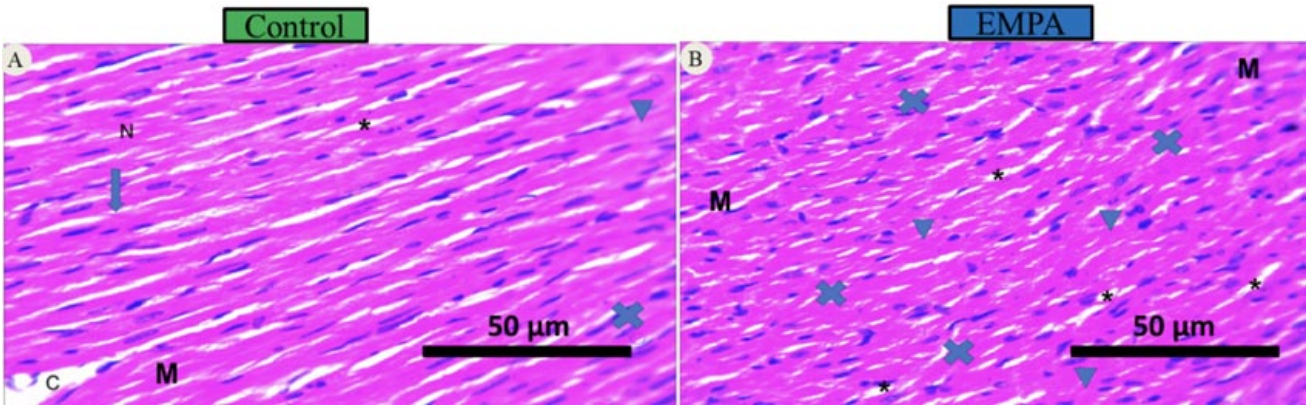


Fig. 3. (A) Photomicrograph of the left ventricle from a control adult male rat displaying bundles of branching and anastomosing cardiomyocytes (M) separated by narrow spaces (*). The cardiomyocytes have a regular outline (blue arrow) and acidophilic sarcoplasm. (Blue x). The sarcoplasm exhibits visible cross-striations (inverted blue triangle), with a single vesicular nucleus (N). Spaces between muscle bundles contain normal blood capillaries (C). (H&E, x 400, scale bar 50 µm). (B) Photomicrograph of the left ventricle from an adult male rat treated with empagliflozin, showing nearly normal bundles of branching and anastomosing cardiomyocytes (M), separated by narrow spaces (*). The cardiomyocytes have a regular outline (blue arrow), appear smaller, and have more acidophilic sarcoplasm than normal (Blue x). The sarcoplasm shows visible cross-striations (inverted blue triangle), with small, apparently normal nuclei (N), and wider intercellular spaces compared to the control group (C). (H&E, x 400, scale bar 50 µm).

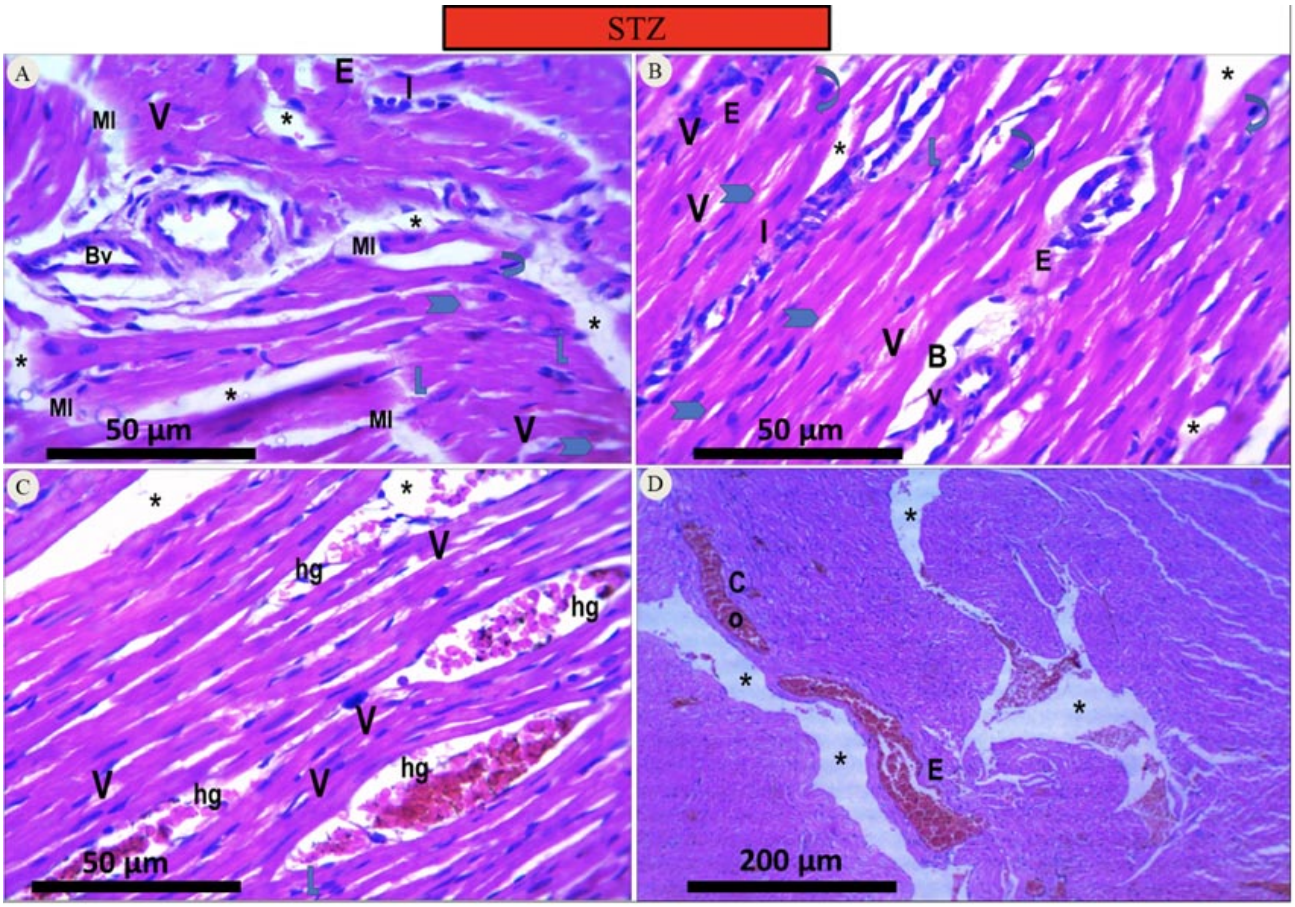


Fig. 4. (A-D) Photomicrographs of the left ventricle of an adult male rat from the STZ group showing disrupted myocardial architecture with widened spaces (*) between abnormal muscle fibers (MI). Inflammatory exudate (E), extensive hemorrhage (hg), and severe congestion (Co) are observed, along with focal interstitial mononuclear cell infiltration (I). Blood vessels (Bv) and capillaries are visible between cardiomyocytes. Many cardiomyocytes show splitting of fibers (MI), vacuolated pale sarcoplasm (V), and dark-stained nuclei (curved arrows). Some nuclei display margination of chromatin (L-shaped), and others show a boxcar appearance (Bc). There are apoptotic nuclei indicative of Zucker degeneration (bifid arrow). (A to C H&E, x 400; scale bar for D is 50 µm, for D with scale bar 200 µm).

Table IV. Effects of Empagliflozin on Histological Features of Myocardial Fibrosis, Cardiomyocyte Hypertrophy, and Structural Remodeling in STZ-Induced Cardiac Injury in Rats Across All Study Groups.

Histopathological parameters	Control	EMPA	STZ	STZ+EMPA	*P* value
Myocardial fibrosis	0(0-0)	0(0-0)	4(3-4)^{a,b}	1(1-2)^{a,b,c}	<0.001
Interstitial fibrosis	0(0-0)	0(0-0)	3(3-3)^{a,b}	1(1-1)^{a,b,c}	<0.001
Cardiomyocyte hypertrophied, wavy-directed, and spitted	0(0-0)	1(1-1)^{a}	2(2-2)^{a,b}	2(1-2)^{a,b}	<0.001
Widened spaces & Inflammatory exudate	0(0-0)	1(1-1)^{a}	4(3-4)^{a,b}	2(1-2)^{a,b}	<0.001
Extensive hemorrhage (hg) and severe congestion	0(0-0)	0(0-0)	4(3-4)^{a,b}	2(1-2)^{a,b}	<0.001
Dark-stained nuclei, nuclei display margination of chromatin (L-shaped), and others show a boxcar appearance (Bc)	0(0-0)	1(1-1)^{a}	4(3-4)^{a,b}	2(1-2)^{a,b}	<0.001

Data are expressed in the form of the second interquartile range (Quartile 3- Quartile 1) for each group. The number of examined fields is 10 for each group. statistically non-significant (p>0.05).

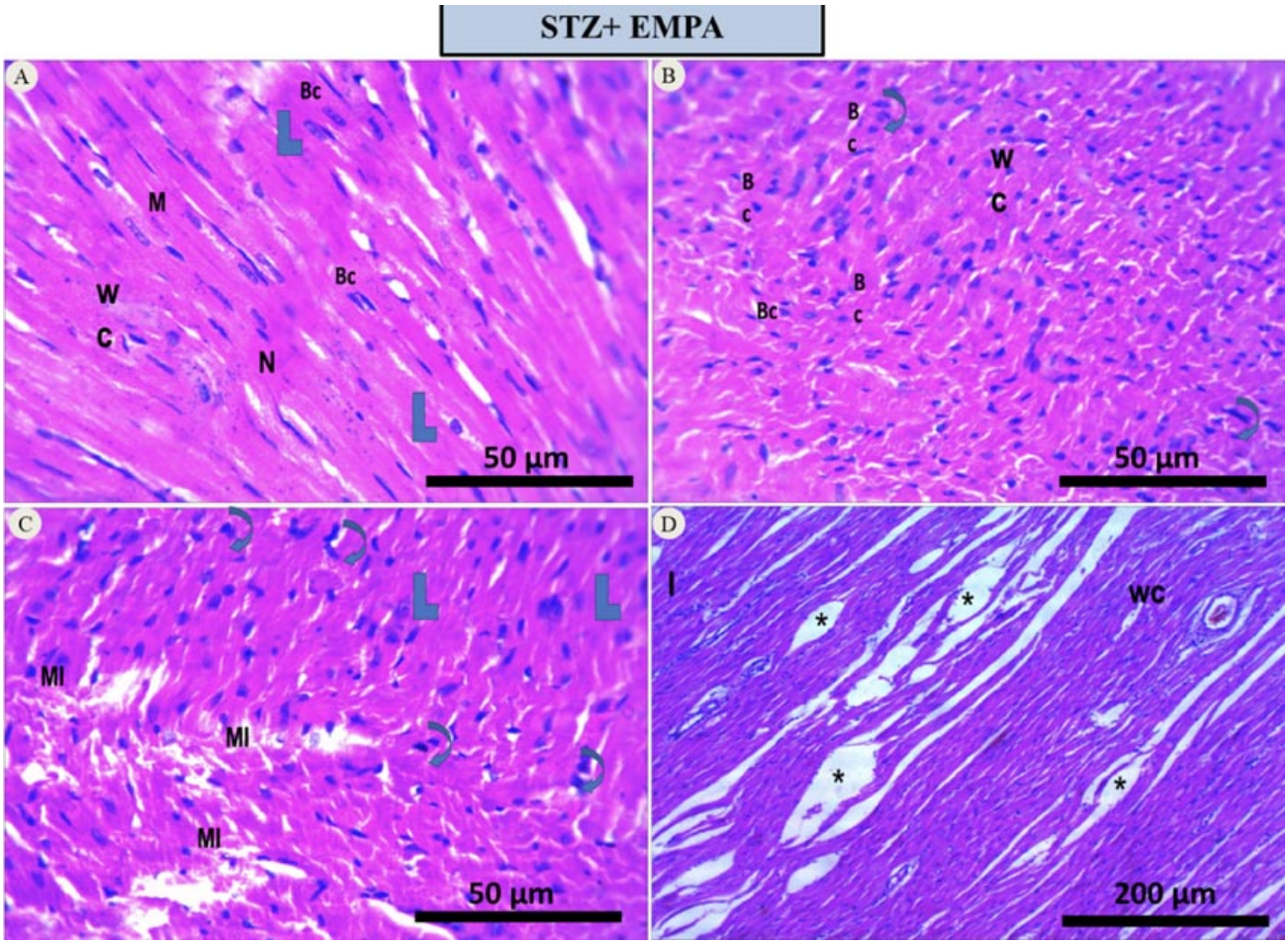


Fig. 5. (A-D) Photomicrographs of the left ventricle from an adult diabetic male rat treated with empagliflozin, showing slightly widened spaces (*). Moderate splitting of cardiomyocytes (MI), with inflammatory cellular infiltrates (I) between irregular, wavy-directed cardiomyocytes (Wc). Nuclei display margination of chromatin (L-shaped), with others stained darkly (curved arrows). (A to CH&E, x 400; scale bar 50 µm, and D with scale bar 200 µm).

which in turn alters indices such as superoxide dismutase (SOD) activity and malondialdehyde (MDA) levels as the antioxidant system attempts to compensate. Progressive disruption of cardiomyocyte membrane integrity and permeability ultimately favors the development of necrotic lesions within the myocardium.

Parallel to these biochemical alterations, endogenous radical-scavenging systems, such as superoxide dismutase (SOD) and related markers of lipid peroxidation, are mobilized to limit oxidative damage at the cellular level (Tawfik *et al*., 2016). These antioxidant enzymes are pivotal in modulating oxidative stress during cardiac injury, and their dysregulation is particularly evident in diabetes, as experimental diabetic mouse models exhibit markedly exacerbated oxidative stress (Li *et al*., 2019).

The present study demonstrated that oxidative stress biomarkers were markedly elevated in untreated diabetic groups, whereas empagliflozin administration substantially reduced these indices in treated animals. Notably, in Group 2 (empagliflozin alone), wider interfibrillar spaces were observed relative to controls, suggesting subtle structural modulation. These findings align with the cardioprotective profile of empagliflozin described by Yang & Zhang (2023), who reported that this SGLT2 inhibitor enhances cardiac function, limits myocardial injury, and improves cardiovascular prognosis in patients with diabetes.

Empagliflozin acts in the kidney by inhibiting the sodium–glucose cotransporter 2, thereby reducing proximal tubular reabsorption of both glucose and sodium (Wiviott *et al*., 2019). In the present work, histological and immunohistochemical assessment demonstrated intense

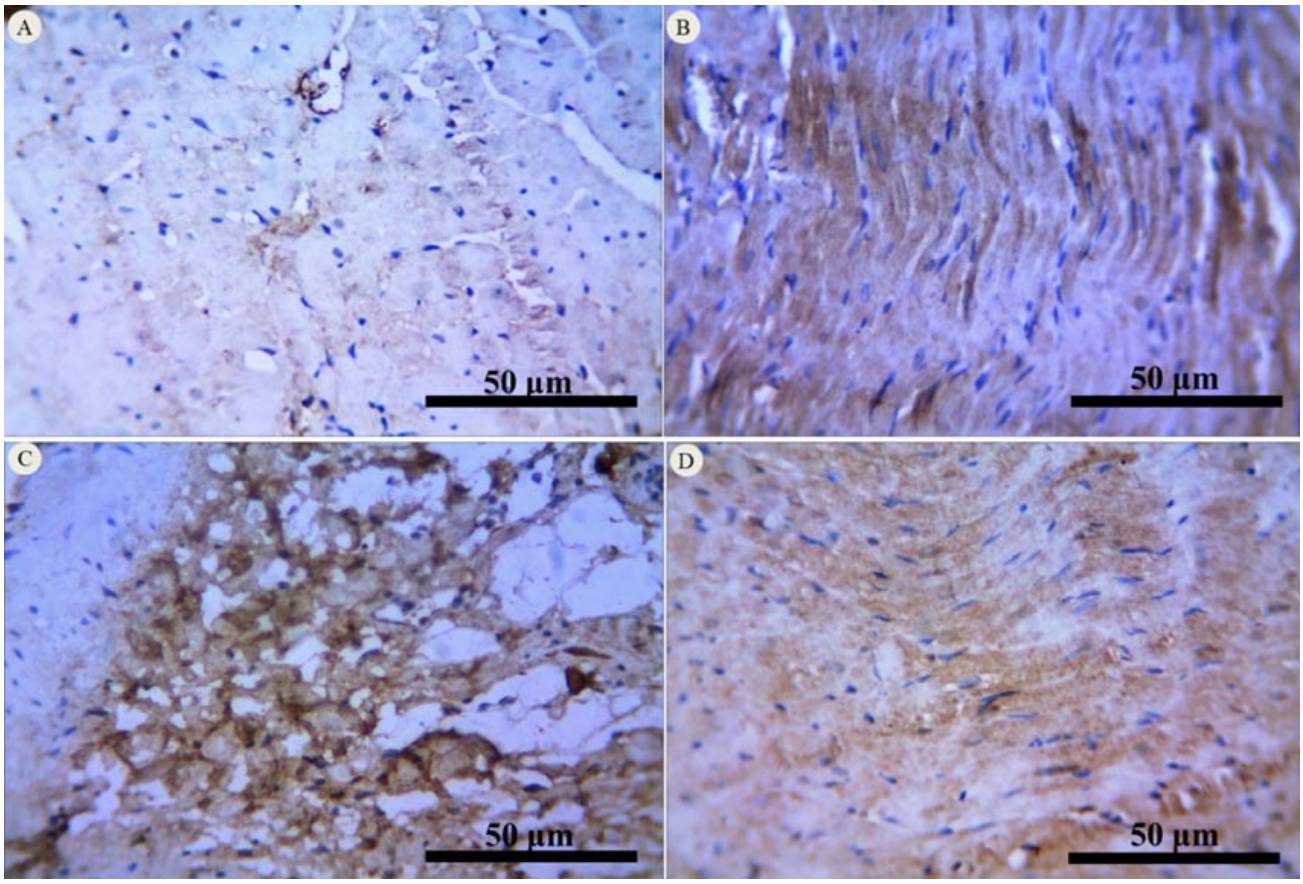


Fig. 6. (A-D). Photomicrographs of the left ventricle from adult male rats in different groups, stained for aquaporin. There is minimal reaction in the control group, mild in the EMPA group, severe in the STZ group, and moderate in the STZ+EMPA group

brown labeling for aquaporin and a-SMA in the diabetic group, contrasting with the weak or absent staining observed in control and empagliflozin-treated animals. This pattern is consistent with experimental data indicating that altered aquaporin expression modulates astrocyte migration and water homeostasis, contributing to astrogliosis and edema in inflammatory and ischemic conditions (Mader & Brimberg, 2019; Sun *et al*., 2022). Furthermore, models with aquaporin inhibition have shown suppression of glucose-induced cell swelling, underscoring the role of these channels at the interface of water and glucose dynamics (Tirado-García *et al*., 2025).

Disruption of a-smooth muscle actin (a-SMA) organization has been linked to vascular wall pathology, including smooth muscle cell hyperplasia, disordered collagen architecture, and fragmentation of elastic fibers, changes that are accompanied by abnormally intense a-SMA expression in aortic disease states (Yuan & Wu, 2018; Dye *et al*., 2020). In the present work, gene expression profiling focused on two key axes: mitochondrial quality control via mitophagy (Prkn) and glucose homeostasis signaling (MEN1). Prkn expression was significantly altered, with a global reduction across diabetic groups relative to non-diabetic controls—consistent with prior observations of mitophagy impairment in hyperglycemic settings (Song *et al*., 2022)—and a notable upregulation in response to empagliflozin treatment.

The anti-diabetic action of empagliflozin, particularly its glucose-lowering and organ-protective effects, appears closely linked to modulation of Prkn-dependent mitophagy (Zhu *et al*., 2024). Earlier studies have shown that Prkn plays a central role in tagging and removing damaged mitochondria; sustained high-glucose exposure suppresses Prkn expression and disrupts glycolipid metabolism, thereby aggravating mitochondrial injury (Li *et al*., 2020). In diabetic nephropathy, such mitochondrial dysfunction is typified by reduced mitochondrial membrane potential and impaired respiratory chain activity, which together amplify oxidative stress and tissue damage (Zhao *et al*., 2020).

The present findings are consistent with earlier work on metformin, which has been shown to confer

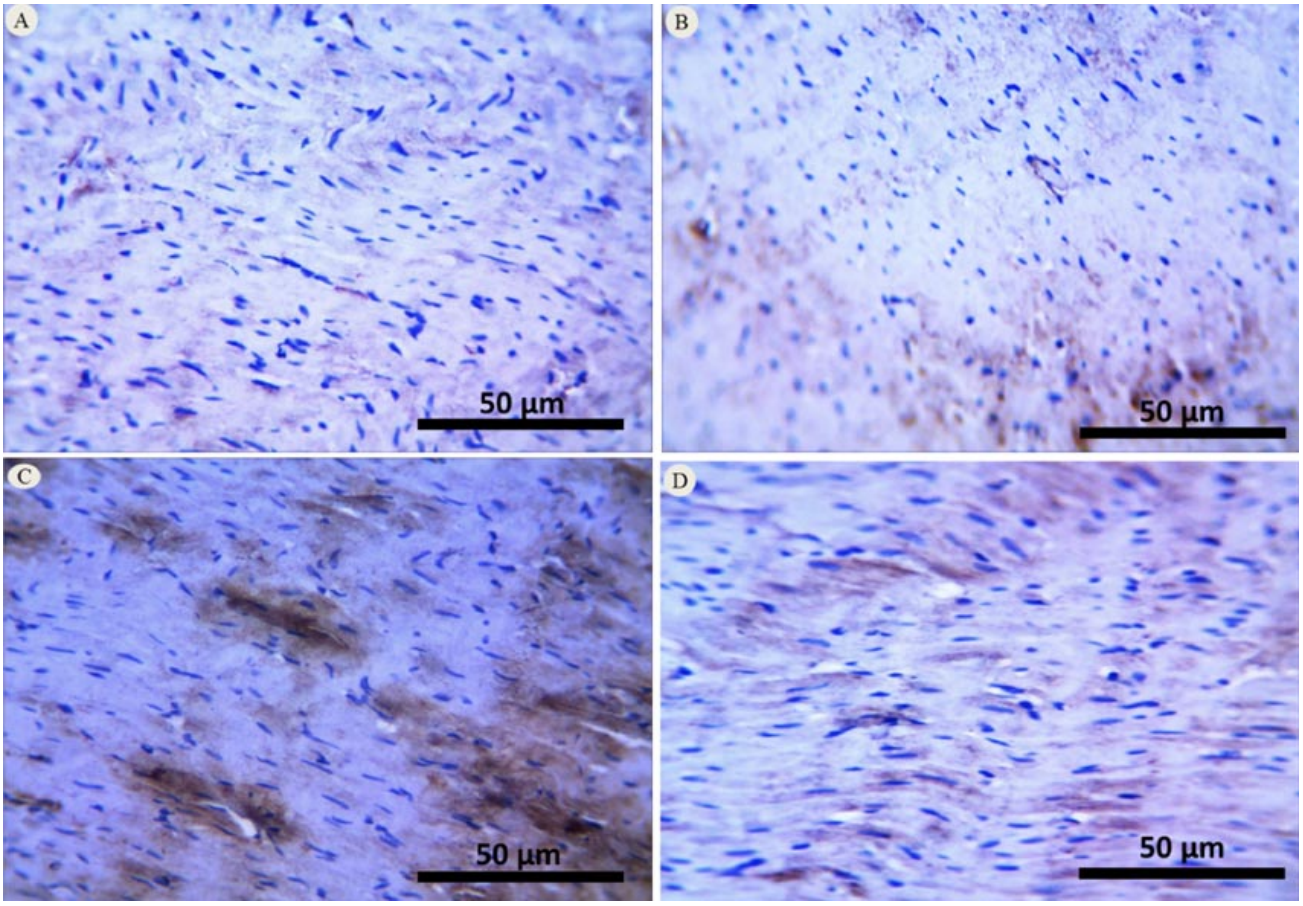


Fig. 7. (A-D). Photomicrographs of the left ventricle from adult male rats across different study groups, stained for a-smooth muscle actin, showing minimal reaction in the control group, mild in the EMPA group, severe in the STZ group, and moderate in the STZ+EMPA group.

cardioprotection, in part, by preserving mitochondrial homeostasis in diabetic settings (Zhao *et al*., 2020). Notably, our data highlight a distinct pattern of Prkn modulation, suggesting that the sustained cardioprotective effect of chronic empagliflozin treatment may be mediated by stabilization of mitochondrial membrane potential and maintenance of ATP production (Choi *et al*., 2023). Together, these molecular changes align with the observed biochemical and immunohistochemical improvements and further support empagliflozin as a potent anti-diabetic agent with clinically relevant benefits for patients with cardiovascular disease.

Collectively, these data reinforce the idea that targeting mitochondrial quality control and oxidative–inflammatory signaling offers tangible structural and functional benefits in the diabetic heart. By integrating gene expression, biochemical, and immunohistochemical evidence, this work positions empagliflozin not only as a glucose-lowering drug but also as a cardiometabolic modulator with the potential to slow disease progression in high-risk patients. Further longitudinal and mechanistic studies, particularly in human populations, are necessary to determine the optimal timing for treatment, clarify tissue-specific effects, and identify the best strategies for incorporating empagliflozin into comprehensive cardioprotective approaches.

Ethics approval statement. The experiments were conducted in compliance with the National Institutes of Health's guide for the care and use of laboratory animals, the U.K. Animals (Scientific Procedures) Act, international ethical standards, and ARRIVE recommendations. The research methodology and animal studies were authorized by Zagazig University's College of Medicine's Ethics Committee for Animal Experimentation guidelines (Approval number: ZU-IACUC/1/F/185/2025).

Conflicts of interest. The authors declare that they have no conflict of interest.

ACKNOWLEDGMENTS. Princess Nourah bint Abdulrahman University Researchers Supporting Project number (PNURSP2026R774), Princess Nourah bint Abdulrahman University, Riyadh, Saudi Arabia.

Artificial Intelligence (AI) Disclosure. The authors used the Nano Banana Gemini Pro to assist with the conceptual design and technical rendering of the study illustrations. It was used solely for visual representation purposes. After generating these assets, the authors critically reviewed, edited, and validated the illustrative content to ensure scientific accuracy.

ELSAWY, N. A.; SHAHEEN, S.; SALEH, A.; DAHRAN, N. A.; ALGIFRY, H.A.; ELKATTAWY, H. A.; ALI, S. K.; NAGUIB, R.; SOLIMAN, N.M.M. & ALGAZEERY, A. La empagliflozina atenúa el daño cardíaco en ratas diabéticas inducidas por STZ mediante la modulación de las acuaporinas y la actina alfa de músculo liso. *Int. J. Morphol., 44(4)*:1448-1460, 2026.

RESUMEN: La diabetes mellitus (DM) es un trastorno metabólico crónico caracterizado por hiperglucemia persistente, que conduce a un daño progresivo en múltiples órganos. Entre las complicaciones graves, la miocardiopatía diabética (MCD) se reconoce cada vez más como un factor importante en la mortalidad cardiovascular asociada a la diabetes. Los inhibidores del cotransportador sodio-glucosa tipo 2 (SGLT2), como la empagliflozina (EMP), están bien establecidos como agentes hipoglucemiantes; sin embargo, sus mecanismos protectores directos sobre el tejido cardíaco aún no se comprenden completamente. Este estudio tuvo como objetivo explorar las funciones cardio protectoras y de modulación molecular de la EMP en un modelo de rata con MCD. Cuarenta ratas albinas macho (180–200 g) se dividieron en cuatro grupos (n=10): control, vehículo, diabético y diabético tratado con EMP (10 mg/kg/día) durante ocho semanas. Los tejidos cardíacos se analizaron histológica e inmunohistoquímicamente para determinar la expresión de acuaporinas y actina alfa de músculo liso (a-SMA). Los cambios moleculares se evaluaron adicionalmente cuantificando la expresión del gen Prkn, un regulador clave de la mitofagia. El tratamiento con empagliflozina mejoró notablemente la histoarquitectura cardíaca y redujo los biomarcadores de estrés oxidativo en comparación con las ratas diabéticas no tratadas. El análisis inmunohistoquímico reveló una disminución significativa en la expresión de acuaporinas y α-SMA. Además, el tratamiento con EMP aumentó la expresión de ARNm de Prkn, lo que indica una mayor actividad de mitofagia en los cardiomiocitos. La empagliflozina ejerce un efecto cardioprotector distintivo en ratas diabéticas mediante la modulación de los canales de acuaporina, la remodelación del citoesqueleto y la mitofagia mediada por Prkn. Estos hallazgos aportan nuevos conocimientos mecanísticos sobre los beneficios cardíacos directos de la inhibición de SGLT2, respaldando a EMP como una diana terapéutica prometedora para la miocardiopatía diabética.

PALABRAS CLAVE: Miocardiopatía diabética; Inhibidor de SGLT2; Empagliflozina; Acuaporina; α-SMA; Mitofagia; Prkn.

REFERENCES

Agre, P. Aquaporin water channels. *Biosci. Rep., 24(3)*:127-63, 2004.

Bancroft, J. D. & Cook, H. C. *Manual of Histological Techniques*. Edinburgh, Churchill Livingstone, 1984.

Bertero, E.; Prates Roma, L.; Ameri, P. & Maack, C. Cardiac effects of SGLT2 inhibitors: the sodium hypothesis. *Cardiovasc. Res., 114(1)*:12-18, 2018.

Balakrishnan, B.; Somashekara, D. M.; Nayak, V. & Hariharapura, R. C. Diabetic cardiomyopathy: a comprehensive review of diagnosis, management, and future directions. *Diabetol. Metab. Syndr., 17(1)*:422, 2025.

Bogdanffy, M. S.; Stachlewitz, R. F.; van Tongeren, S.; Knight, B.; Sharp, D. E.; Ku, W.; Hart, S. E. & Blanchard, K. Nonclinical safety of the sodium-glucose cotransporter 2 inhibitor empagliflozin. *Int. J. Toxicol., 33(6)*:436-49, 2014.

Choi, J.; Matoba, N.; Setoyama, D.; Watanabe, D.; Ohnishi, Y.; Yasui, R.; Kitai, Y.; Oomachi, A.; Kotobuki, Y.; Nishiya, Y.; *et al*. The SGLT2 inhibitor empagliflozin improves cardiac energy status via mitochondrial ATP production in diabetic mice. *Commun. Biol., 6(1)*:278, 2023.

Dye, B. K.; Butler, C. & Lincoln, J. Smooth muscle actin expression in mitral valve interstitial cells is important for mediating extracellular matrix remodeling. *J. Cardiovasc. Dev. Dis., 7(3)*:32, 2020.

Egan, J. R.; Butler, T. L.; Au, C. G.; Tan, Y. M.; North, K. N. & Winlaw, D. S. Myocardial water handling and the role of aquaporins. Biochim. *Biophys. Acta, 1758(8)*:1043-52, 2006.

Ekici, M.; Güngör, H.; Karayıgˇıt, M. Ö.; Turgut, N. H.; Koçkaya, M.; Karatas¸, Ö. & Üner, A. G. Cardioprotective effect of empagliflozin in rats with isoproterenol-induced myocardial infarction: evaluation of lipid profile, oxidative stress, inflammation, DNA damage, and apoptosis. *Biol. Bull., 49(Suppl. 1)*:S159-72, 2022.

Elkattawy, H. A.; Elsherbini, D. M.; Ebrahim, H. A.; Abdullah, D. M.; Al-Zahaby, S. A.; Noser, Y. & Hassan, A. E. Rho-kinase inhibition ameliorates non-alcoholic fatty liver disease in type 2 diabetic rats. *Physiol. Res., 71(5)*:615-30, 2022.

Elkattawy, H. A.; Alsemeh, A. E.; Ali, L. S.; Ahmed, M. M.; Eltaweel, A. M.; Shaikh, F. M.; Behiry, A.; Hassan, A. E.; Sabir, D. K.; Elsherbini, D. M. A.; *et al*. Decorin alleviates non-alcoholic fatty liver disease in rats with polycystic ovary syndrome. *Tissue Cell, 93*:102689, 2025.

Elkattawy, H. A.; Mahmoud, S. M.; Hassan, A. E.; Behiry, A.; Ebrahim, H. A.; Ibrahim, A. M.; Zaghamir, D. E. F.; El-Sherbiny, M. & El-Sayed, S. F. Vagal stimulation ameliorates non-alcoholic fatty liver disease in rats. *Biomedicines, 11(12)*:3255, 2023.

Furman, B. L. Streptozotocin-induced diabetic models in mice and rats. *Curr. Protoc., 1(4)*:e78, 2021.

Gheibi, S.; Kashfi, K. & Ghasemi, A. A practical guide for induction of type-2 diabetes in rats: incorporating a high-fat diet and streptozotocin. *Biomed. Pharmacother., 95*:605-13, 2017.

Ghezzi, C.; Loo, D. D. F. & Wright, E. M. Physiology of renal glucose handling via SGLT1, SGLT2, and GLUT2. *Diabetologia, 61(10)*:2087-97, 2018.

Hassan, A. E.; Hadhoud, S.; Elmahdi, E. & Elkattawy, H. A. Potential cardioprotective role of menaquinone-4 against cardiac ischemia-reperfusion injury. *J. Cardiovasc. Pharmacol., 81(5)*:381-8, 2023.

Hirayama, B. A.; Wong, H. C.; Smith, C. D.; Hagenbuch, B. A.; Hediger, M. A. & Wright, E. M. Intestinal and renal Na+/glucose cotransporters share common structures. *Am. J. Physiol., 261(2 Pt. 1)*:C296-304, 1991.

Joost, H. G. & Thorens, B. The extended GLUT-family of sugar/polyol transport facilitators: nomenclature, sequence characteristics, and potential function of its novel members (review). *Mol. Membr. Biol., 18(4)*:247-56, 2001.

Kakkar, P.; Das, B. & Viswanathan, P. N. A modified spectrophotometric assay of superoxide dismutase. *Indian J. Biochem. Biophys., 21(2)*:130-2, 1984.

Koay, Y. C.; McIntosh, B.; Ng, Y. H.; Cao, Y.; Wang, X. S.; Han, Y.; Tomita, S.; Bai, A. Y.; Hunter, B.; Misra, A.; *et al*. The heart has intrinsic ketogenic capacity that mediates NAD+ therapy in HFpEF. *Circ. Res., 136(10)*:1113-30, 2025.

Koepsell, H. Glucose transporters in brain in health and disease. *Pflugers Arch., 472(9)*:1299-343, 2020.

Li, C.; Zhang, J.; Xue, M.; Li, X.; Han, F.; Liu, X.; Xu, L.; Lu, Y.; Cheng, Y.; Li, T.; *et al*. SGLT2 inhibition with empagliflozin attenuates myocardial oxidative stress and fibrosis in diabetic mice heart. *Cardiovasc. Diabetol., 18(1)*:15, 2019.

Li, Y.; Chen, D.; Xu, C.; Zhao, Q.; Ma, Y.; Zhao, S. & Chen, C. Glycolipid metabolism and liver transcriptomic analysis of the therapeutic effects of pressed degreased walnut meal extracts on type 2 diabetes mellitus rats. *Food Funct., 11(6)*:5538-52, 2020.

Livak, K. J. & Schmittgen, T. D. Analysis of relative gene expression data using real-time quantitative PCR and the 2-DDCT method. *Methods, 25(4)*:402-8, 2001.

Loscalzo, J.; Fauci, A. S.; Kasper, D. L.; Hauser, S. L.; Longo, D. L. & Jameson, J. L. (Eds.). *Harrison's Principles of Internal Medicine*. 21st ed. New York, McGraw Hill, 2022.

Mackey, A. L.; Magnan, M.; Chazaud, B. & Kjaer, M. Human skeletal muscle fibroblasts stimulate *in vitro* myogenesis and in vivo muscle regeneration. *J. Physiol., 595(15)*:5115-27, 2017.

Mader, S. & Brimberg, L. Aquaporin-4 water channel in the brain and its implication for health and disease. *Cells, 8(2)*:90, 2019.

Masaebi, F.; Salehi, M.; Kazemi, M.; Vahabi, N.; Azizmohammad Looha, M. & Zayeri, F. Trend analysis of disability adjusted life years due to cardiovascular diseases: results from the global burden of disease study 2019. *BMC Public Health, 21(1)*:1268, 2021.

Matthews, D. R.; Hosker, J. P.; Rudenski, A. S.; Naylor, B. A.; Treacher, D. F. & Turner, R. C. Homeostasis model assessment: insulin resistance and beta-cell function from fasting plasma glucose and insulin concentrations in man. *Diabetologia, 28(7)*:412-9, 1985.

Mohamad, Y. R.; Hany, A. E. & Rania, A. F. Plasma asprosin levels change in pregnant and non-pregnant rats with and without gestational diabetes. *Int. J. Med. Res. Health Sci., 9(3)*:54-63, 2020.

Mueckler, M. Facilitative glucose transporters. *Eur. J. Biochem., 219(3)*:713-25, 1994.

Ohkawa, H.; Ohishi, N. & Yagi, K. Assay for lipid peroxides in animal tissues by thiobarbituric acid reaction. *Anal. Biochem., 95(2)*:351-8, 1979.

Oliver, I. T. A spectrophotometric method for the determination of creatine phosphokinase and myokinase. *Biochem. J., 61(1)*:116-22, 1955.

Pang, D. & Laferriere, C. Review of intraperitoneal injection of sodium pentobarbital as a method of euthanasia in laboratory rodents. *J. Am. Assoc. Lab. Anim. Sci., 59(3)*:346, 2020.

Rosalki, S. B.; Roberts, R.; Katus, H. A.; Giannitsis, E.; Ladenson, J. H. & Apple, F. S. Cardiac biomarkers for detection of myocardial infarction: perspectives from past to present. *Clin. Chem., 50(11)*:2205-13, 2004.

Rutkovskiy, A.; Valen, G. & Vaage, J. Cardiac aquaporins. *Basic Res. Cardiol., 108(6)*:393, 2013.

Samuel, V. T.; Liu, Z. X.; Wang, A.; Beddow, S. A.; Geisler, J. G.; Kahn, M.; Zhang, X. M.; Monia, B. P.; Bhanot, S. & Shulman, G. I. Inhibition of protein kinase Ce prevents hepatic insulin resistance in nonalcoholic fatty liver disease. *J. Clin. Invest., 117(3)*:739-45, 2007.

Sanjari, M.; Hadavizadeh, M.; Sadeghi, N. & Naghibzadeh-Tahami, A. Effect of empagliflozin on weight in patients with prediabetes and diabetes. *Sci. Rep., 15(1)*:118, 2025.

Scheepers, A.; Joost, H. G. & Schürmann, A. The glucose transporter families SGLT and GLUT: molecular basis of normal and aberrant function. *JPEN J. Parenter. Enteral Nutr., 28(5)*:364-71, 2004.

Song, Y.; Nie, L.; Wang, M.; Liao, W.; Huan, C.; Jia, Z.; Wei, D.; Liu, P.; Fan, K.; Mao, Z.; *et al*. Differential expression of lncRNA-miRNA-mRNA and their related functional networks in new-onset type 2 diabetes mellitus among Chinese rural adults. *Genes (Basel), 13(11)*:2073, 2022.

Song, H.; Tian, X.; Liu, D.; Liu, M.; Liu, Y.; Liu, J.; Mei, Z.; Yan, C. & Han, Y. CREG1 improves the capacity of the skeletal muscle response to exercise endurance via modulation of mitophagy. *Autophagy, 17(12)*:4102-18, 2021.

Steven, S.; Oelze, M.; Hanf, A.; Kröller-Schön, S.; Kashani, F.; Roohani, S.; Welschof, P.; Kopp, M.; Gödtel-Armbrust, U.; Xia, N.; *et al*. The SGLT2 inhibitor empagliflozin improves the primary diabetic complications in ZDF rats. *Redox Biol., 13*:370-85, 2017.

Sun, C.; Lin, L.; Yin, L.; Hao, X.; Tian, J.; Zhang, X.; Ren, Y.; Li, C. & Yang, Y. Acutely inhibiting AQP4 with TGN-020 improves functional outcome by attenuating edema and peri-infarct astrogliosis after cerebral ischemia. *Front. Immunol., 13*:870029, 2022.

Tawfik, M.; Al-Aleem, A.; Ibrahim, R. & Abaza, R. Effect of nesfatin-1 on ischaemia-reperfusion injury in isolated heart of albino rats. Zagazig *Univ. Med. J., 22(6)*:1-11, 2016.

Tie, L.; Wang, D.; Shi, Y. & Li, X. Aquaporins in cardiovascular system. *Adv. Exp. Med. Biol., 969*:105-13, 2017.

Tirado-García, P.; Ferreiro, A.; González-Alday, R.; Arias-Ramos, N.; Lizarbe, B. & López-Larrubia, P. Aquaporin-4 inhibition alters cerebral glucose dynamics predominantly in obese animals: an MRI study. *Sci. Rep., 15(1)*:15649, 2025.

Warade, J. P. & Pandey, A. Fasting blood glucose level higher than post-meal in healthy subjects: a study of 738 subjects. *World J. Pharm. Res., 3(4)*:1121-8, 2014.

Wiviott, S. D.; Raz, I.; Bonaca, M. P.; Mosenzon, O.; Kato, E. T.; Cahn, A.; Silverman, M. G.; Zelniker, T. A.; Kuder, J. F.; Murphy, S. A.; *et al*. Dapagliflozin and cardiovascular outcomes in type 2 diabetes. *N. Engl. J. Med., 380(4)*:347-57, 2019.

Wood, I. S. & Trayhurn, P. Glucose transporters (GLUT and SGLT): expanded families of sugar transport proteins. *Br. J. Nutr., 89(1)*:3-9, 2003.

Wright, E. M. Renal Na(+)-glucose cotransporters. Am. J. Physiol. Renal Physiol., 280(1):F10-8, 2001.

Yang, T. & Zhang, D. Research progress on the effects of novel hypoglycemic drugs in diabetes combined with myocardial ischemia/reperfusion injury. *Ageing Res. Rev., 86*:101884, 2023.

Yuan, T.; Yang, T.; Chen, H.; Fu, D.; Hu, Y.; Wang, J.; Yuan, Q.; Yu, H.; Xu, W. & Xie, X. New insights into oxidative stress and inflammation during diabetes mellitus-accelerated atherosclerosis. *Redox Biol., 20*:247-60, 2019.

Yuan, S. M. & Wu, N. Aortic a-smooth muscle actin expressions in aortic disorders and coronary artery disease: an immunohistochemical study. *Anatol. J. Cardiol., 19(1)*:11-6, 2018.

Zhao, Y. & Sun, M. Metformin rescues Parkin protein expression and mitophagy in high glucose-challenged human renal epithelial cells by inhibiting NF-kB via PP2A activation. *Life Sci., 246*:117382, 2020.

Zhu, J. Y.; van de Leemput, J. & Han, Z. Promoting mitochondrial dynamics by inhibiting the PINK1–PRKN pathway to relieve diabetic nephropathy. *Dis. Model. Mech., 17(4)*:dmm050471, 2024.

Corresponding author:
Hany A. Elkattawy
College of Medicine
Al Maarefa University
Diriyah 13713
Riyadh
SAUDI ARABIA

E-mail: hmohammed@um.edu.sa
skamal@um.edu.sa

Corresponding author:
Ahmed Algazeery
Zoology Department
Zagazif University
EGYPT

E-mail: asalgazeery@zu.edu.eg